Available online at www.sciencedirect.com

ScienceDirect

IFAC Papers Online
CONFERENCE PAPER ARCHIVE

IFAC-PapersOnLine 49-13 (2016) 070–075

Reference-dependent variable-gain control for a nano-positioning motion system ⋆

S.J.L.M. van Loon * **B.G.B. Hunnekens** * **A.S. Simon** *
N. van de Wouw *,** **W.P.M.H. Heemels** *

* *Mechanical Engineering Department, Eindhoven University of Technology, the Netherlands*

Abstract: In this paper, we develop a variable-gain (VG) control strategy that allows for a reference-dependent 'bandwidth' of the feedback controller. The proposed controller architecture can achieve improved performance given time-varying, reference-dependent performance requirements compared to linear time-invariant control, which suffers from design trade-offs between low-frequency tracking performance and sensitivity to higher-frequency disturbances. The VG controller consists of frequency-domain loop-shaped linear filters and a VG element. The gain of this element depends on reference information and determines the desired reference-dependent bandwidth of the resulting controller. We present data-based frequency-domain conditions to verify stability and convergence of the closed-loop system. The complete controller design process and the ability of the 'bandwidth-on-demand' controller to outperform linear time-invariant controllers are illustrated through experiments on an industrial nano-positioning motion system.

Keywords: Variable-gain control; bandwidth; performance; experiments.

1. INTRODUCTION

The increasing performance demands on speed, accuracy, throughput, etc., of today's high-precision motion systems require them to operate under diverse modes of operation, each related to a distinct set of performance requirements. If this comes with the presence of multiple disturbance sources, active in various frequency ranges, this poses a challenging control design task. This is due to the fact that the vast majority of controller designs techniques employed in the scope of motion control generally relies on classical linear control theory in which fundamental design trade-offs are inherently present. Namely, increasing the bandwidth of the controlled system improves the low-frequency disturbance rejection properties, and, hence, the tracking-performance, but due to the waterbed effect, this also results in a larger sensitivity to higher-frequency disturbances (i.e., around and/or above the bandwidth), see, e.g., Seron et al. (1997). This fundamental trade-off can already be challenging when just one mode of operation is considered, but this is severely aggravated when high performance is required in multiple modes of operation because this generally means that the control objectives vary over time, e.g., depend on the reference. Due to fundamental limitations in linear time-invariant (LTI) feedback control, the design of one LTI controller typically requires a compromise between these conflicting design goals thereby limiting the overall performance achievements of the controlled system.

In this paper, we propose a variable-gain (VG) control strategy that allows for a reference-dependent, and thus time-varying, 'bandwidth' of the feedback controller. By taking on-line reference information into account, this feature allows the controller to 'anticipate' on the required 'bandwidth' for each mode of operation. This allows, contrary to LTI control, to deal with the conflicting control objectives induced by reference-dependent dominance of multiple disturbance sources that are acting in various frequency ranges. The proposed controller consists of frequency-domain loop-shaped linear filters and a VG element, with its gain depending on reference information and inducing the desired 'bandwidth' of the resulting controller. The proposed controller structure supports the design of all the linear components of the VG controller configuration using well-known (frequency-domain) loop-shaping techniques, see, e.g., Steinbuch and Norg (1998). It therefore connects to the state-of-the-art industrial motion control setting, in which easy-to-measure frequency response functions (FRFs) play an important role in the controller design, e.g., by using frequency-domain loop-shaping techniques. This is in contrast to many other techniques that can deal with the considered trade-off, such as linear parameter varying (LPV) control, see, e.g., Groot Wassink et al. (2005); Shamma and Athans (1991) and switched controller design, see, e.g., Hespanha and Morse (2002); Liberzon (2003), which require accurate parametric models and LMI-based designs that are not so easily embraced by control engineers in industry.

The concept of VG control has already been successfully applied in numerous industrial applications to improve the performance of (linear) motion systems, see, e.g.,

⋆ This research is financially supported by the Dutch Technology Foundation (STW) under the project "HyperMotion: Hybrid Control for Performance Improvement of Linear Motion Systems" (no. 10953).

** N. van de Wouw is also with the Department of Civil, Environmental and Geo-Engineering, University of Minnesota, Minneapolis, MN 55455 USA, and also with the Delft Center for Systems and Control, Delft University of Technology, Delft, The Netherlands e-mail: {s.j.l.m.v.loon, b.g.b.hunnekens, a.s.simon, n.v.d.wouw,m.heemels}@tue.nl

10.1016/j.ifacol.2016.07.929

Hunnekens et al. (2014); Zheng et al. (2005); van de Wouw et al. (2008); Heertjes et al. (2009); Armstrong et al. (2001). In fact, the use of VG control to target similar LTI control design trade-offs as considered in this paper, i.e., balancing trade-offs between low-frequency tracking properties and sensitivity to higher-frequency disturbances, has been considered in e.g., van de Wouw et al. (2008); Heertjes et al. (2009). The novelty in our approach lies in the fact that we couple this fundamental trade-off to time-varying control objectives depending on on-line reference information, which makes it possible to design a time-varying controller with a 'bandwidth-on-demand' characteristic.

Summarizing, the main contributions of this paper are as follows. Firstly, a novel reference-dependent VG control strategy is introduced that has a 'bandwidth-on-demand' characteristic. Secondly, graphical data-based conditions to verify stability and convergence of the VG controlled closed-loop system are presented. Thirdly, the entire design process and its potential to outperform LTI controllers are experimentally demonstrated on an industrial case study of a nano-positioning motion stage.

1.1 Nomenclature

The following notational conventions will be used. Let $\mathbb{C}, \mathbb{R}$ denote the set of complex and real numbers, respectively, and $\mathbb{R}^n$ denote the space of n-dimensional vectors with the standard Euclidean norm denoted by $\|\cdot\|$. The real part of a complex variable z is denoted by $Re(z)$. The Laplace transform of a signal $x : \mathbb{R}_{\geq 0} \to \mathbb{R}^n$ is denoted by $\mathfrak{L}\{x\}$ and $s \in \mathbb{C}$ denotes the Laplace variable.

Moreover, let us make precise what is meant by bandwidth given its prominent role in this paper. Consider therefore the linear feedback control configuration in Fig. 1 with linear plant $\mathcal{P}(s)$, $s \in \mathbb{C}$, and a linear controller $\mathcal{C}(s)$. The bandwidth ω_b is defined as the frequency $\omega \in \mathbb{R}^+$, where the magnitude of the open-loop $|\mathcal{P}(j\omega)\mathcal{C}(j\omega)|$ crosses 1 from above for the first time, see, e.g., Skogestad and Postlethwaite (2005). By definition, bandwidth is a linear time-invariant (LTI) concept and, hence, does not apply to our proposed time-varying control strategy. Nevertheless, with abuse of definition, we will use the term 'bandwidth' in this paper (to indicate the bandwidth of the linear controller underlying the proposed strategy) but use quotation marks to avoid confusion with the LTI case. Moreover, from this point onward we sometimes use the terms 'low-bandwidth/high-bandwidth' controller to denote a controller that results in a low/high bandwidth, respectively.

2. SYSTEM DESCRIPTION AND PROBLEM FORMULATION

The nano-positioning motion system considered in this paper is an experimental setup of a high-precision motion

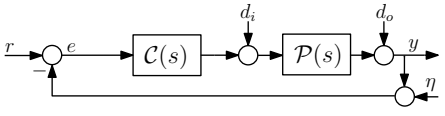

Fig. 1. Schematic representation of a classical LTI feedback controlled system.

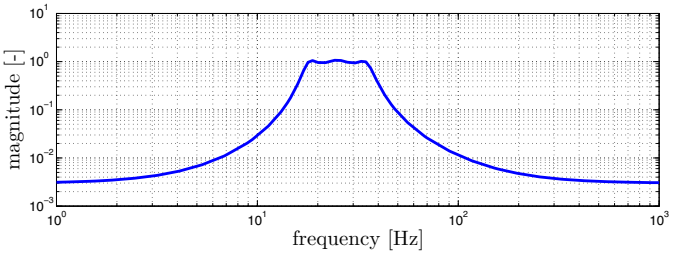

Fig. 2. Bode magnitude plot of the filter $\mathcal{H}(j\omega)$.

system that requires movements with velocities ranging from standstill, to nanometers per second (nm/s), to even millimeters per second (mm/s), all with (sub)nanometer resolution. The nano-positioning motion system has several key modes of operation, namely: (i) standstill, (ii) constant velocities in a broad range, and (iii) fast (user-operated) point-to-point movements. We will show that due to the presence of multiple disturbance sources in various frequency ranges (depending also on the mode of operation), this results in conflicting control design trade-offs when using LTI control.

2.1 Nano-positioning motion stage

The nano-positioning motion system is driven by piezoelectric actuators, positioned on a vibration isolation table and equipped with a 1^{st}-order 100 Hz low-pass actuation filter $\mathcal{P}_{act}(s)$ in the hardware to filter off high-frequency actuator noise. Based on measured frequency response functions, it is known that, firstly, the plant $\mathcal{P}_n(j\omega)$ behaves as a rigid-body system in the frequency range of interest, and secondly, the presence of a significant, and thus bandwidth-limiting, delay.

Consider Fig. 1, in which the plant is given by $\mathcal{P}(s) = \mathcal{P}_n(s)\mathcal{P}_{act}(s)$. Based on identification [1], the following disturbances are acting on the system: Sensor noise η, modeled as white noise with zero mean and variance $\lambda_\eta^2 = (10^{-9})^2$, actuator noise $d_{i,act}$ modeled as white noise with zero mean and variance $\lambda_{d_{i,act}}^2 = (\sqrt{10^{-19}})^2$, and periodic impact disturbances $d_{i,p}$ (induced by piezoelectric actuators) that depend on the reference velocity v. Moreover, because the experimental nano-positioning motion setup operates in a lab-environment instead of in its dedicated application, additional environmental disturbances are emulated to recover the real situation in the application as much as possible. Based on measurement data, an output disturbance $d_{o,add} = \mathcal{H}(s)\varepsilon$ has been identified, where the magnitude of $\mathcal{H}(j\omega)$ is depicted in Fig. 2 and ε is normally distributed white noise with zero mean and variance $\lambda_\varepsilon^2 = (2 \cdot 10^{-9})^2$.

2.2 Problem formulation

Let us now study the control design trade-off in a model-based environment, in which $\mathcal{P}_n(s)$ represents a 2^{nd}-order LTI model identified based on measured FRF data. In

[1] To protect the interests of the manufacturer, we can not provide concrete information about the disturbance modeling and the reference velocities (and thus scheduling variables v to be introduced later). For the same reason, most figures in this paper have either been scaled or use blank axes in terms of units.

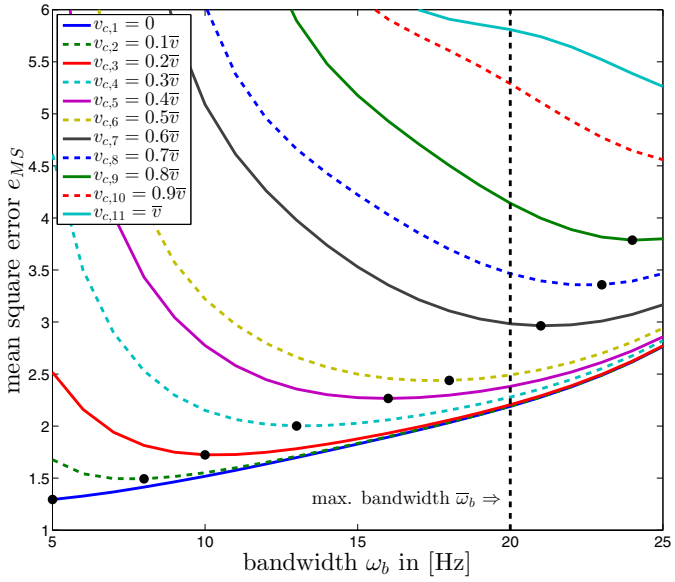

Fig. 3. Mean square closed-loop error e_{MS}, at various constant reference velocities $v_{c,i}$ as a function of the bandwidth ω_b. The black dots denote the optimal bandwidth $\omega_{b,opt,i}$ for each $v_{c,i}$, $i = 1, 2, \ldots, 11$.

order to do so, a range of constant reference velocities $v_{c,i}$, $i = 1, 2, \ldots, 11$, are created in the set $v_{c,i} \in [0, \overline{v}]$, and 21 LTI controllers $\mathcal{C}_j(s)$ are designed each having a different bandwidth $\omega_{b,j}$, $j = 1, 2, \ldots, 21$. These controllers all consist of the same types of linear filters, namely a lead filter, integrator and 2^{nd}-order low-pass filter, and are given by

$$\mathcal{C}_j(s) = k_{p,j} \left\{ \frac{s + 2\pi f_{I,j}}{s} \right\} \left\{ \frac{\frac{1}{2\pi f_{le1,j}} s + 1}{\frac{1}{2\pi f_{le2,j}} s + 1} \right\} \times \left\{ \frac{1}{\frac{1}{(2\pi f_{l,j})^2} s^2 + \frac{1}{2\pi f_{l,j}} s + 1} \right\}, \quad (1)$$

in which $f_{le1,j} = \frac{1}{4}\omega_{b,j}$, $f_{le2,j} = 4\omega_{b,j}$, $f_{I,j} = \frac{1}{9}\omega_{b,j}$, $f_{l,j} = 6\omega_{b,j}$, which all depend on the bandwidth $\omega_{b,j}$, $j = 1, 2, \ldots, 21$. By shaping the gains $k_{p,j}$ to appropriate values, 21 controllers with different bandwidths $\omega_{b,j} \in [5, 25]$ Hz, $j = 1, 2, \ldots, 21$, have been designed. By taking the performance measure J as the mean square of the error, which is given for an $N \times 1$ vector e of measured error data by $e_{MS} := \frac{1}{N} \sum_{i=1}^{N} |e_i|^2$, the performance as a function of the bandwidth for each constant reference $v_{c,i}$, $i = 1, 2, \ldots, 11$, is characterized and depicted in Fig. 3. This shows us that the 'optimal bandwidth' $\omega_{b,opt,i}$ increases for increasing reference velocities $v_{c,i}$, $i = 1, 2, \ldots, 11$, which results in an inevitable trade-off when using LTI control to design a controller that should service all reference velocities.

3. REFERENCE-DEPENDENT VG CONTROL

In this section, a reference-dependent VG control strategy with a 'bandwidth-on-demand' characteristic is proposed.

3.1 Description of the control configuration

The overall reference-dependent feedback control configuration as proposed in this paper is shown in Fig. 4. It consists of a standard LTI feedback controlled system,

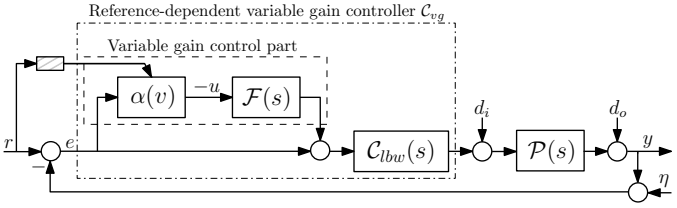

Fig. 4. Schematic representation of the reference-dependent VG controlled system.

similar as in Fig. 1 (in which the nominal LTI controller $\mathcal{C}(s) = \mathcal{C}_{lbw}(s)$), augmented with an add-on variable gain control part. This variable gain part of the total controller $\mathcal{C}_{vg}$ consists of an LTI shaping filter $\mathcal{F}(s)$, and a time-varying variable gain $\alpha(v(t))$ depending on a *scheduling variable* $v(t)$, $t \in \mathbb{R}_{\geq 0}$, which is related to characteristics of the reference signal. In this paper, and in particular in Section 5, we will use the reference velocity as scheduling variable, i.e., $v(t) = \dot{r}(t)$, although other options are imaginable as well. For instance, the variable gain could depend on the reference position, i.e., $v(t) = r(t)$, on the acceleration, i.e., $v(t) = \ddot{r}(t)$, etc. The process of extracting the relevant information, e.g., $v(t) = \dot{r}(t)$, from the reference signal r is indicated by the dashed box in Fig. 4. Note that for the particular choices mentioned, the reference information is not required to be known in advance. The variable gain element is given by a mapping $\alpha : \mathbb{R} \to [0, \bar{\alpha}]$, where $\bar{\alpha} \in \mathbb{R}_{>0}$ denotes the maximum gain value. Let us first consider the situation where $\alpha \in [0, \bar{\alpha}]$ is a *fixed* gain, and study the following cases ($\alpha = 0$ and $\alpha \in (0, \bar{\alpha}]$):

- If $\alpha = 0$, we have a linear control scheme with linear controller $\mathcal{C}_{vg}^f(s) = \mathcal{C}_{lbw}(s)$;
- For a *fixed* $\alpha \in (0, \bar{\alpha}]$, we have a linear control scheme with controller

$$\mathcal{C}_{vg}^f(s) = (1 + \alpha \mathcal{F}(s)) \mathcal{C}_{lbw}(s). \quad (2)$$

Remark 1. The reference-dependent VG controller reduces only to an LTI controller for fixed values of α. Therefore, we denote it by $\mathcal{C}_{vg}^f(s)$ only when α is *fixed*, and use $\mathcal{C}_{vg}$ with $\alpha(v(t))$ varying over time otherwise.

The introduction of the variable gain element allows us to deal with the conflicting design criteria as described in the introduction and discussed in Section 2.2, i.e., preferring a controller that results in a low bandwidth $\underline{\omega}_b$ over a controller that results in a higher bandwidth $\underline{\omega}_b < \omega_b \leq \overline{\omega}_b$, or vise versa, *depending on actual reference information.* In fact, by assigning $\alpha(v(t)) = 0$ to the situation where a low bandwidth is preferable, the user can loop-shape the controller $\mathcal{C}_{lbw}(s)$ such that the best possible performance is obtained for this particular situation. On the other hand, the proposed structure of the reference-dependent VG controller $\mathcal{C}_{vg}$ allows that, by proper design of the variable gain element $\alpha : \mathbb{R} \to [0, \bar{\alpha}]$ and the linear filter $\mathcal{F}(s)$ (see below in Section 5.1), the 'bandwidth' ω_b of the VG controller $\mathcal{C}_{vg}^f(s)$ (for fixed values of α) will gradually increase (and can take values in $[\underline{\omega}_b, \overline{\omega}_b]$) for increasing values of $\alpha \in [0, \bar{\alpha}]$.

The system as in Fig. 4 belongs to the class of Lur'e-type systems, see, e.g., Khalil (2000), as depicted schematically in Fig. 5. Such systems consist of a linear dynamical part

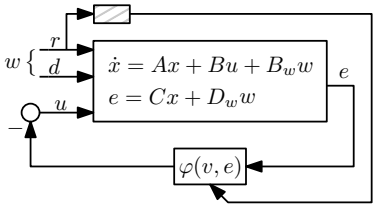

Fig. 5. Schematic representation of a Lur'e-type description of the reference-dependent VG controlled system.

in feedback with with a time-varying, but memoryless, variable gain element given (in this case) by $\varphi(v(t), e)$. Consider therefore Fig. 5, in which the linear part is given by

$$\mathfrak{L}\{e\} = \mathcal{G}_{eu}(s)\mathfrak{L}\{u\} + \mathcal{G}_{ew}(s)\mathfrak{L}\{w\}, \tag{3}$$

where the external inputs are denoted by $w = [r \;\; d^\top]^\top \in \mathbb{R}^{n_w}$, with reference input $r \in \mathbb{R}$ and a vector $d = [d_i^\top \;\; d_o^\top \;\; \eta]^\top \in \mathbb{R}^{n_d}$ containing the external disturbances. In (3), the transfer function between 'input' u and 'output' e, see Fig. 5, is given by

$$\mathcal{G}_{eu}(s) = \mathcal{F}(s) \underbrace{\frac{\mathcal{P}(s)\mathcal{C}_{lbw}(s)}{1 + \mathcal{P}(s)\mathcal{C}_{lbw}(s)}}_{=:\mathcal{T}(s)}, \tag{4}$$

in which $\mathcal{T}(s)$ represents the complementary sensitivity function, and the transfer function between the external inputs w and e is given by

$$\mathcal{G}_{ew}(s) = \left[\mathcal{S}(s) \;\; -\mathcal{S}_p(s) \;\; -\mathcal{S}(s) \;\; -\mathcal{S}(s)\right], \tag{5}$$

in which $\mathcal{S}(s)$ and $\mathcal{S}_p(s)$ represent the sensitivity and process sensitivity function, respectively. The closed-loop dynamics can be represented in state-space form as

$$\dot{x} = Ax + Bu + B_w w \tag{6a}$$
$$e = Cx + D_w w \tag{6b}$$
$$u = -\varphi(v, e) \tag{6c}$$

with state $x \in \mathbb{R}^{n_x}$, (A, B, C) minimal such that $\mathcal{G}_{eu}(s) = C(sI - A)^{-1}B$, and $\mathcal{G}_{ew}(s) = C(sI - A)^{-1}B_w + D_w$ with I an identity matrix of appropriate dimensions. Finally, the variable gain in Fig. 5 depends on the reference via

$$\varphi(v, e) = \alpha(v)e, \tag{7}$$

for all $v \in \mathbb{R}$ and $e \in \mathbb{R}$.

4. DATA-BASED STABILITY CONDITIONS

In this section, we present data-based graphical conditions to verify stability and convergence (Demidovich (1961); Pavlov et al. (2006)) of the closed-loop system (6) with variable gain $\varphi(v, e)$ given by (7) for every $\alpha : \mathbb{R} \to [0, \bar{\alpha}]$ and any choice of scheduling variable v. Let us therefore provide a formal definition of a convergent system by considering a general nonlinear system description of the form

$$\dot{x} = f(x, w, t) \tag{8}$$

with state $x \in \mathbb{R}^{n_x}$ and input $w \in \mathbb{R}^{n_w}$. The function $f(x, w, t)$ is locally Lipschitz in x, continuous in w and piecewise continuous in t. Moreover, the inputs $w(t)$ are assumed to be piecewise continuous functions of time defined for all $t \in \mathbb{R}$.

Definition 2. Demidovich (1961); Pavlov et al. (2006) System (8) is said to be

- *convergent* if there exists a solution $\bar{x}_w(t)$ such that
  - (i) $\bar{x}_w(t)$ is defined for all $t \in \mathbb{R}$ and bounded for all $t \in \mathbb{R}$,
  - (ii) $\bar{x}_w(t)$ is globally asymptotically stable;
- *exponentially convergent* if it is convergent and $\bar{x}_w(t)$ is globally exponentially stable.

In Definition 2, the solution $\bar{x}_w(t)$ (which depends on the input $w(t)$) denotes the steady-state solution of the system (8). It states that any solution of a convergent system converges to a bounded steady-state solution, independent of its initial conditions. For exponentially convergent systems, this steady-state solution is also unique, see Pavlov et al. (2006). Being able to ensure convergence of the VG controlled system (6), (7) is advantageous from a stability, a performance and a design point-of-view. Namely, convergence implies, firstly, stability for any reference and disturbance realization and, secondly, the existence of a unique steady-state solution. The latter property allows for a unique steady-state performance evaluation in the presence of disturbances, and, as such, it also results in an easier design and tuning of the VG controller $\mathcal{C}_{vg}$. The following conditions are sufficient to establish that a system of the form (6), (7) is exponentially convergent.

Theorem 3. Consider system (6) with variable gain $\varphi(v, e)$ given by (7), in which $\alpha : \mathbb{R} \to [0, \bar{\alpha}]$ for all $t \in \mathbb{R}$ for some $\bar{\alpha} \in \mathbb{R}_{>0}$. Suppose that

(I) The system matrix A is Hurwitz;
(II) The frequency response function $\mathcal{G}_{eu}(j\omega)$ as in (4) satisfies

$$\frac{1}{\bar{\alpha}} + Re(\mathcal{G}_{eu}(j\infty)) > 0, \tag{9}$$

and

$$\frac{1}{\bar{\alpha}} + Re(\mathcal{G}_{eu}(j\omega)) > 0 \quad \text{for all} \;\; \omega \in \mathbb{R}. \tag{10}$$

Then, system (6), (7) is exponentially convergent.

Remark 4. Condition (I) of Theorem 3 will be satisfied by proper controller design of $\mathcal{C}_{lbw}(s)$. This is due to the fact that if the open-loop $\mathcal{P}(s)\mathcal{C}_{lbw}(s)$ satisfies the Nyquist stability criterion, see, e.g., Skogestad and Postlethwaite (2005), the complementary sensitivity function $\mathcal{T}(s)$ has all its poles located in the complex left half plane (LHP). In addition, if the shaping filter $\mathcal{F}(s)$ is designed such that it has no unstable poles, the transfer function $\mathcal{G}_{eu}(s)$ as in (4) will have all its poles located in the LHP as well. As a result, the system matrix A of (6) will be a Hurwitz matrix. Moreover, note that for many motion systems $\mathcal{G}_{eu}(j\omega) \to 0$ for $\omega \to \infty$, resulting in condition (9) being satisfied automatically. Nevertheless, satisfying (10) is not trivial and generally requires the design and tuning of an appropriate shaping filter $\mathcal{F}(s)$.

5. CASE-STUDY ON AN INDUSTRIAL NANO-POSITIONING MOTION SYSTEM

In this section, we design a reference-dependent VG controller for the nano-positioning motion system as discussed in Section 2.1. Due to space reasons, we only briefly comment on the design and refer to van Loon (2016) for more details.

5.1 Design of a reference-dependent VG controller

The total design process comprises the following steps: **Step 1**: *Design of an LTI low-bandwidth and high-*

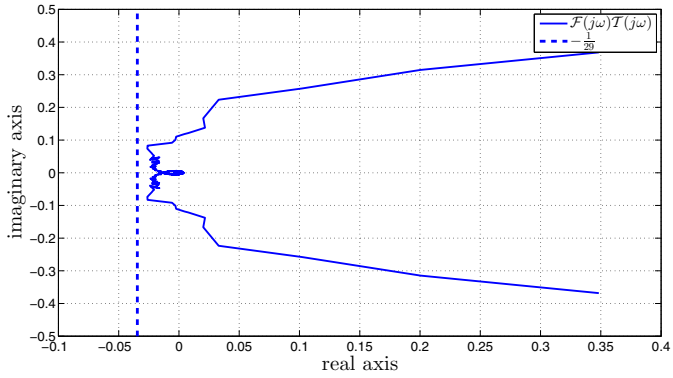

Fig. 6. Nyquist diagram for $\mathcal{G}_{eu}(j\omega)$ as in (4) with shaping filter $\mathcal{F}(s)$ as in (12), showing that the circle criterion condition $Re(\mathcal{F}(j\omega)\mathcal{T}(j\omega)) > -\frac{1}{\bar{\alpha}}$, is met for all $\omega \in \mathbb{R}$ with $\bar{\alpha} = 29$.

bandwidth controller $\mathcal{C}_{lbw}(s)$ and $\mathcal{C}_{hbw}(s)$, respectively.
Based on Fig. 3, we select the desired low bandwidth $\underline{\omega}_b$ as $\underline{\omega}_b = \min_{i=1,2,\ldots,n} \omega_{b,opt,i} = 5$ Hz and design the corresponding LTI controller $\mathcal{C}_{lbw}(s)$. The LTI controller $\mathcal{C}_{hbw}(s)$ is designed such that the highest achievable bandwidth $\overline{\omega}_b$ is obtained under sufficient robustness margins, resulting in a controller that achieves a bandwidth of $\overline{\omega}_b = 20$ Hz.

Step 2: *Design the linear filter $\mathcal{F}(s)$ and determine the maximum allowable gain $\bar{\alpha}$.*
In this step we will design $\mathcal{F}(s)$ and $\bar{\alpha}$ with the aim to vary the 'bandwidth' ω_b of the resulting controller $\mathcal{C}_{vg}$ on-line in the set $[5, 20]$, depending on the scheduling variables v. The control architecture of the proposed VG controller as in Fig. 4 results in $\mathcal{C}^f_{vg}(s) = \mathcal{C}_{lbw}(s)$ for the limit case $\alpha = 0$. For the other limit case, $\alpha = \bar{\alpha}$, we aim to design $\mathcal{F}(s)$, and determine $\bar{\alpha}$, such that

$$(1 + \bar{\alpha}\mathcal{F}(s))\mathcal{C}_{lbw}(s) \approx \mathcal{C}_{hbw}(s), \tag{11}$$

which results in the filter

$$\mathcal{F}(s) = \left\{\frac{\frac{1}{2\pi 26}s+1}{\frac{1}{2\pi 105}s+1}\right\}\left\{\frac{\frac{1}{2\pi 30}s+1}{\frac{1}{2\pi 110}s+1}\right\}^2\left\{\frac{\frac{1}{2\pi 6}s+1}{\frac{1}{2\pi 0.5}s+1}\right\} \times \left\{\frac{\frac{1}{(2\pi 26.5)^2}s^2 + \frac{2\cdot 0.85}{2\pi 26.5}s+1}{\frac{1}{(2\pi 80)^2}s^2 + \frac{2\cdot 1.3}{2\pi 80}s+1}\right\}. \tag{12}$$

Based on the circle criterion condition (10), the maximal gain is selected as $\bar{\alpha} = 29$, thereby allowing for some robustness margin, see Fig. 6, which shows that the solid red line stays on the right of the dashed-red line with some margin. Once the circle criterion condition (10) has been verified, i.e., $Re(\mathcal{G}_{eu}(j\omega)) > -\frac{1}{29}$ for all $\omega \in \mathbb{R}$, and realizing that $\mathcal{G}_{eu}(j\omega) \to 0$ for $\omega \to \infty$, condition (II) of Theorem 3 is satisfied. In order to verify condition (I), note that the low-bandwidth controller $\mathcal{C}_{lbw}(s)$ is designed such that the open-loop $\mathcal{P}_n(s)\mathcal{P}_{act}(s)\mathcal{C}_{lbw}(s)$ satisfies the Nyquist stability criterion, see, e.g., Skogestad and Postlethwaite (2005). Since the shaping filter $\mathcal{F}(s)$ has no unstable poles, we also satisfy condition (I) of Theorem 3, see Remark 4. Hence, we can conclude that all conditions of Theorem 3 are being satisfied, which guarantees that the designed reference-dependent VG controlled system is exponentially convergent, independent of how the gain $\alpha(v(t)) \in [0, 29]$, $t \in \mathbb{R}_{\geq 0}$, varies over time.

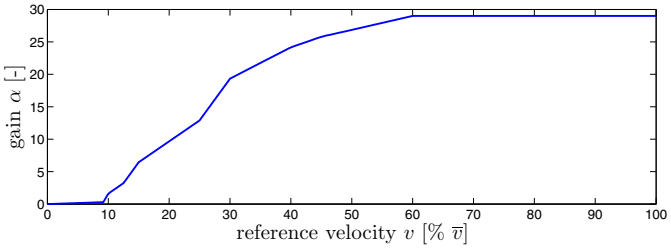

Fig. 7. The relationship between the reference velocity v (represented in % of $\overline{v}$) and α.

Step 3: *Design the 'reference-to-gain' mapping $\alpha : [\underline{v}, \overline{v}] \to [0, 29]$.*
The last step in the design of a reference-dependent VG controller $\mathcal{C}_{vg}$ is to design the mapping $\alpha : [\underline{v}, \overline{v}] \to [0, 29]$, which for this cases study results in Fig. 7.

5.2 Experimental results

Let us start with presenting the results of the performance analysis of the measured steady-state error e, depicted in Fig. 8. The analysis is performed for constant reference velocities $v(t) = v_c$, for all $t \in \mathbb{R}_{\geq 0}$, using the two linear controllers $\mathcal{C}_{lbw}(s)$ and $\mathcal{C}_{hbw}(s)$ and the reference-dependent VG controller $\mathcal{C}^f_{vg}(s)$ as in (2) for different *fixed* values of $\alpha \in [0, 29]$. Note that for each velocity v_c there exists a corresponding optimal $\alpha \in [0, 29]$, see Fig. 7. Let us first focus on low velocities v_c in the range $[0, 0.1\overline{v}]$, see the zoom plot in Fig. 8. Clearly, in this range both the low-bandwidth controller $\mathcal{C}_{lbw}(s)$ as well as the reference-dependent VG controller $\mathcal{C}^f_{vg}(s)$ perform better than the high-bandwidth controller $\mathcal{C}_{hbw}(s)$ as their mean square error e_{MS} is significantly lower (at $v_c = 0$) or, at worst, (approximately) equal (at $v_c = 0.1\overline{v}$). At standstill, we achieve (approximately) the same performance with the VG controller $\mathcal{C}^f_{vg}(s)$ (with $\alpha = 0$) as for $\mathcal{C}_{lbw}(s)$, while compared to $\mathcal{C}_{hbw}(s)$, the performance is deteriorated by $\sim 66\%$. This is due to the fact that for this case, the disturbances $d_{o,add}$, $d_{i,a}$ and η are being dominant, which are more amplified in the high-bandwidth situation.

Fig. 8 also demonstrates that the higher the reference velocity v_c, the more beneficial it is to have a higher bandwidth controller. This is due to the fact that for increasing reference velocities the periodic disturbance d_p due to the piezo-electric actuator becomes more influential and eventually dominant over $d_{o,add}$, $d_{i,a}$ and η. The effect of this disturbance is suppressed by increasing the gain α and, as a result, the increasing 'bandwidth' ω_b of the VG controller $\mathcal{C}_{vg}$. With this in mind, let us now focus in Fig. 8 on the velocities v_c in the range $[0.1\overline{v}, \overline{v}]$. As expected, the low-bandwidth controller $\mathcal{C}_{lbw}(s)$ performs worst, since its bandwidth of 5 Hz is too low to suppress the periodic impact disturbances d_p caused by the piezo actuators. The high-bandwidth controller $\mathcal{C}_{hbw}(s)$ and our reference-dependent VG controller $\mathcal{C}^f_{vg}(s)$ show an approximately similar performance, which is superior compared to that of $\mathcal{C}_{lbw}(s)$.

The previous results were obtained for constant reference velocities, resulting in fixed values of α and, hence, a comparison between $\mathcal{C}_{lbw}(s)$ and $\mathcal{C}_{hbw}(s)$ with a linear controller $\mathcal{C}^f_{vg}(s)$. However, it is ultimately more important

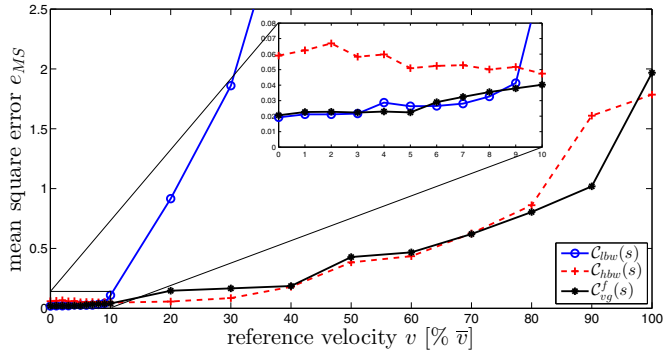

Fig. 8. Performance measure of the measured steady-state error e of the nano-motion system for 20 constant velocities v_c in the range $[0, \overline{v}]$ (in % of $\overline{v}$).

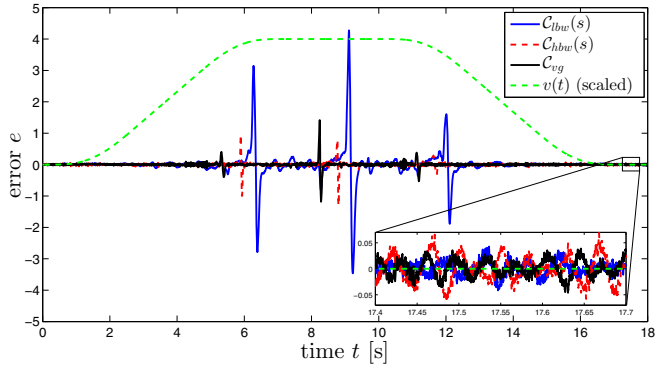

Fig. 9. Time-domain performance analysis, moving from $v(t) = 0$ to $v(t) = \overline{v}$ with a constant acceleration, and back to $v(t) = 0$.

to compare the behavior for *time-varying* velocity profiles, which is depicted in Fig. 9. This figure shows the time-domain error behavior for a constant acceleration, starting from $v(t) = 0$ until we move at $v(t) = \overline{v}$ for approximately 5 sec, and then moving back to $v(t) = 0$. Indeed, as indicated in Fig. 9, the performance using $\mathcal{C}_{vg}$ for low velocities is comparable with using $\mathcal{C}_{lbw}(s)$ (see the zoom at the end of the setpoint), while for high velocities the performance of $\mathcal{C}_{vg}$ is similar to $\mathcal{C}_{hbw}(s)$. This demonstrates that the proposed reference-dependent VG controller $\mathcal{C}_{vg}$ is able to deal with reference-dependent conflicting control design trade-offs. In fact, the experiments show that the VG controller $\mathcal{C}_{vg}$ can achieve 'the best of both worlds', referring to preferring a controller that results in a low bandwidth $\underline{\omega}_b$ over a controller that results in a high bandwidth $\overline{\omega}_b$, or vise versa, depending on the actual reference information.

6. CONCLUSIONS

In this paper, we proposed a novel reference-dependent variable-gain control strategy that allows for a varying 'bandwidth' of the feedback controller in order to deal with reference-dependent conflicting control design trade-offs between low-frequency tracking and high-frequency noise suppression. We showed that most of the design steps involve the usage of frequency-domain loop-shaping tools. This favorable design feature, together with graphical data-based conditions to verify stability and convergence of the variable gain controlled closed-loop system, makes the analysis and design intuitive for control engineers and, as such, connects to the industrial control engineering practice. The design framework has been applied to an industrial nano-positioning motion system with diverse modes of operation. It has been experimentally demonstrated that the proposed reference-dependent variable-gain controller indeed has the ability to outperform (fixed bandwidth) linear time-invariant controllers.

REFERENCES

Armstrong, B., Neevel, D., and Kusik, T. (2001). New results in N-PID control: Tracking, integral control, friction compensation and experimental results. *IEEE Trans. Contr. Syst. Technology*, 9(2), 399–406.

Demidovich, B. (1961). Dissipativity of a nonlinear system of differential equations. *Ser. Mat. Mekh.*, Part I-6, 19–27.

Groot Wassink, M., van de Wal, M., Scherer, C., and Bosgra, O.H. (2005). LPV control for a wafer stage: Beyond the theoretical solution. *Contr. Engineering Practice*, 13(2), 231–245.

Heertjes, M.F., Schuurbiers, X.G.P., and Nijmeijer, H. (2009). Performance-improved design of N-PID controlled motion systems with applications to wafer stages. *IEEE Trans. Indus. Electronics*, 56(5), 1347–1355.

Hespanha, J.P. and Morse, A.S. (2002). Switching between stabilizing controllers. *Automatica*, 38(11), 1905–1917.

Hunnekens, B.G.B., Heertjes, M.F., van de Wouw, N., and Nijmeijer, H. (2014). Performance optimization of piecewise affine variable-gain controllers for linear motion systems. *Mechatronics*, 24(6), 648–660.

Khalil, H.K. (2000). *Nonlinear Systems*. Prentice Hall.

Liberzon, D. (2003). *Switching in systems and control*. Birkhäuser.

Pavlov, A., van de Wouw, N., and Nijmeijer, H. (2006). *Uniform Output Regulation of Nonlinear Systems: A Convergent Dynamics Approach*. Birkhäuser.

Seron, M., Braslavsky, J., and Goodwin, G. (1997). *Fundamental Limitations in Filtering and Control*. Berlin: Springer.

Shamma, J.S. and Athans, M. (1991). Guaranteed properties of gain scheduled control for linear parameter-varying plants. *Automatica*, 27(3), 559–564.

Skogestad, S. and Postlethwaite, I. (2005). *Multivariable Feedback Control: Analysis and Design*. John Wiley & sons, Ltd.

Steinbuch, M. and Norg, M.L. (1998). Advanced motion control: An industrial perspective. *European J. of Control*, 4(4), 278–293.

van de Wouw, N., Pastink, H.A., Heertjes, M.F., Pavlov, A.V., and Nijmeijer, H. (2008). Performance of convergence-based variable-gain control of optical storage drives. *Automatica*, 44(1), 15–27.

van Loon, S. (2016). *Hybrid control for performance improvement of linear systems*. Ph.D. thesis, Eindhoven University of Technology. URL `https://pure.tue.nl/ws/files/13218237/20160126_Loon_van.pdf`.

Zheng, J., Guo, G., and Wang, Y. (2005). Nonlinear PID control of linear plants for improved disturbance rejection. In *16th IFAC World Congress*, volume 16, 281–286.